Numerical Methods for Simulating Neutron Diffusion

Robin Newby*
San Jose State University, Department of Physics and Astronomy, San Jose, CA, USA
(Dated: May 19, 2023)

While the behavior of real nuclear material is highly dependent on neutron energy, the energy-dependent scattering cross sections of fissile nuclei, and the nuclear and radiological properties of decay products, a simplified diffusion model is sufficient for creating a toy model of criticality. Because such a model has a simplified notion of criticality that only takes into account neutrons produced directly from the primary fission process -prompt neutrons- and ignores the delayed neutrons produced by the decays of fission products, it lacks several qualitative behaviors seen in real nuclear systems. Nevertheless, it provides a suitable testing ground for numerical methods.

Keywords: Neutron diffusion, reactor physics, computational methods

I. INTRODUCTION

The neutron diffusion equation approximates the behavior of neutrons in fissile material as a diffusing scalar field $n(x,t)$ with a density-dependent source term Cn.[1]

$$\frac{\partial}{\partial t}n(x,t) = D\nabla^2 n + Cn \tag{1}$$

This model makes a number of simplifying assumptions, some of which are more physically reasonable than others. Initially, the most obvious simplifying assumption is that neutrons go on a random walk through our material, and therefore undergo diffusive transport. This is actually quite reasonable for the neutrons used in reactors, as the neutrons most active in conventional fission reactions are thermal neutrons. Thermal neutrons (in contrast to fast neutrons, those before thermalization) have lost the initial kinetic energy they were created with to the material at large, and have had their direction randomized, allowing for the diffusion approximation to be sensible.

This is consistent with another simplifying assumption: that fission probability is constant for all neutrons we account for. In a real reactor, fast neutrons produced by fissions have a much lower probability of being captured by nuclei and causing fission events than slower, thermal neutrons. [2] By working with only thermal neutrons, we can assume that the neutrons are both acting diffusely (moving on average in no particular direction) and contributing to the fission reaction rate (they are thermal, and are thus captured by nuclei most easily). Still, even working thermal neutrons there is an additional layer of complexity that is important for understanding nuclear reactors.

Our model has a simplified notion of criticality that only takes into account a single type of neutrons produced directly from the primary fission process: prompt neutrons. This ignores the delayed neutrons produced by the decays of fission products, which in real reactors are extremely important for maintaining a controllable reactor. Exactly-critical solutions of the neutron diffusion equation are not stable, as supercriticality causes neutron density to increase without bound, while subcriticality allows for neutron density to decay exponentially in time. In real nuclear reactions, prompt neutrons are not allowed to reach a self-sustaining density (prompt-criticality) as any additional neutrons from decay products would push the system into supercriticality, causing an uncontrolled chain reaction of increasing fission rate. Maximizing the speed and efficiency of this process is the basis for nuclear weapons, and doing so involves managing to increase the reaction rate so quickly and abruptly that a large fraction of the fissionable material undergoes this fission before expanding outwards as a sphere of plasma.

While it is of limited reassurance, it is worth mentioning that it takes great effort to cause a nuclear explosion, and that reactor fuels do not have enough fissionable material to explode in the same way that nuclear weapons do - even during criticality incidents. Catastrophic failures of reactors are instead caused by thermal explosions, where the reactor heats up enough that materials involved in its design rapidly change phase and expand, causing a non-nuclear explosion that is not remotely comparable to a nuclear detonation in energy. Regardless, the timescale at which prompt neutrons cause a doubling of the reaction rate is far too short for outside intervention, meaning that any reactor must reach supercriticality due to an additional source of neutrons produced over a much longer, controllable timescale. [3]

One might imagine a nuclear reactor which is precisely critical, maintaining its neutron flux in a given volume when a control rod is half-inserted. If one wanted to increase this reaction rate to a higher value, but not allow for a reactor-destroying cascade, one might imagine retracting the rod slightly, allowing the neutron flux to increase exponentially for a very short

* Correspondence email address: robert.newby@sjsu.edu

time. The rod would then be inserted to its original position so that the reaction rate stops increasing, but maintains its higher level, producing valuable heat energy for capture via steam. This would not work for a very simple reason: prompt neutrons are too fast for the rod to react. If the reaction were sustained only by prompt neutrons, even a brief excursion to supercriticality would cause exponential power output increases that would cause catastrophic failures of the reactor (a thermal explosion) long before any action could be taken to halt the reaction rate's growth.

To allow for increases in power output, or even any control over the reaction rate at all, a slower process than the action of prompt neutrons is required. As fission products are themselves radioactive, and therefore can produce additional delayed neutrons to aid the reaction, their neutrons are used to bring the reactor into safe excursions above criticality. While the growth in power due to the sum of prompt-and delayed neutrons is still exponential, the timescale of this exponential growth is limited by timescale of the delayed neutrons. [3]

While our model will lack certain qualitative features that only appear when the both prompt and delayed neutrons are accounted for, we can still observe the basic qualitative features of a nuclear chain reaction.[1] For instance, we can imagine choosing values for our neutron creation and diffusion terms that average out the timescale contributions of prompt and delayed neutrons, yielding a coarse description of nuclear behavior.

II. MODEL & METHODS

In this work, we use the FTCS and LAX finite difference methods, where the derivatives of a continuous function are approximated by expressions about grid points on a lattice.[1]

We write the grid point values as

$$n_{i,j}^{n} \tag{2}$$

Where the superscript n signifies time step n, which stands in for real time $t = \tau n$. The spatial location is captured by the subscripts i and j, which stand for grid points along the x and y directions. Their precise relationships to the x and y coordinate systems vary based on the boundary conditions, but regardless they are related to the x and y directions by linear simple equations.

For Dirichlet (fixed-value) boundary conditions, x and y are given by

$$x = ih_x - \frac{L}{2}, \quad y = jh_y - \frac{L}{2} \tag{3}$$

Where h_x and h_y are the size of the gaps between grid points in the x and y directions, and τ is the finite time between time steps.

For Neumann (fixed-derivative) boundary conditions, x and y are given by

$$x = (i - \frac{1}{2})\, h_x - \frac{L}{2}, \quad y = (j - \frac{1}{2})\, h_y - \frac{L}{2} \tag{4}$$

as having points half a space-step from each side of the $\pm\frac{L}{2}$ boundaries allow enforcing derivatives simply by setting values on the edge of the discretized domain.

The FTCS method: Forward time Centered Space, encapsulates the ways we choose to approximate the time and space derivative.

Forward time:

$$\frac{\partial n}{\partial t} \approx \frac{n_{i,j}^{n+1} - n_{i,j}^{n}}{\tau} \tag{5}$$

It is the forward time method because it uses the current time step n and the next time step $n+1$ (the time step that is *forward* in time) to approximate the derivative.

Centered Space: Along the x direction, the second derivative with respect to space would be

$$\frac{\partial^2 n}{\partial x^2} \approx \frac{n_{i+1,j}^{n} + n_{i-1,j}^{n} - 2n_{i,j}^{n}}{h_x^2} \tag{6}$$

with the y direction being written similarly, but with differences in the j index rather than the i one. Since the Laplacian in two dimensions is equal to

$$\nabla^2 = \frac{\partial^2}{\partial x^2} + \frac{\partial^2}{\partial y^2}$$

We can write

$$\nabla^2 n \approx \frac{n_{i+1,j}^{n} + n_{i-1,j}^{n} - 2n_{i,j}^{n}}{h_x^2} + \frac{n_{i,j+1}^{n} + n_{i,j-1}^{n} - 2n_{i,j}^{n}}{h_y^2} \tag{7}$$

Then we can put together the entire diffusion equation

$$\frac{n_{i,j}^{n+1} - n_{i,j}^{n}}{\tau} = D\frac{n_{i+1,j}^{n} + n_{i-1,j}^{n} - 2n_{i,j}^{n}}{h_x^2} + D\frac{n_{i,j+1}^{n} + n_{i,j-1}^{n} - 2n_{i,j}^{n}}{h_y^2} + Cn_{i,j}^{n} \tag{8}$$

[1] One such feature is known as the "prompt jump." In short, the prompt neutrons have a much faster response to changes in environment that affect the reaction rate, so when reactivity increases by, say, removing a control rod, the reaction rate will almost instantly jump to a higher value, then slowly increase further as the delayed neutrons begin to contribute.[3]

Solving for the next time step gives the full FTCS formula for the lattice value at the next time step:

$$n_{i,j}^{n+1} = n_{i,j}^{n} + \tau\Bigg(D\frac{n_{i+1,j}^{n} + n_{i-1,j}^{n} - 2n_{i,j}^{n}}{h_x^2} + D\frac{n_{i,j+1}^{n} + n_{i,j-1}^{n} - 2n_{i,j}^{n}}{h_y^2} + Cn_{i,j}^{n}\Bigg) \quad (9)$$

The LAX method is much the same as the FTCS method, but it replaces all instances of $n_{i,j}^{n}$ with an average of neighboring grid points. In two dimensions, that means the average of four adjacent grid points:

$$n_{i,j}^{n} \longrightarrow \tilde{n}_{i,j}^{n} = \frac{n_{i+1,j}^{n} + n_{i,j+1}^{n} + n_{i-1,j}^{n} + n_{i,j-1}^{n}}{4} \quad (10)$$

Thus, the full equation for the next time step of the LAX method is

$$n_{i,j}^{n+1} = \tilde{n}_{i,j}^{n} + \tau\Bigg(D\frac{n_{i+1,j}^{n} + n_{i-1,j}^{n} - 2\tilde{n}_{i,j}^{n}}{h_x^2} + D\frac{n_{i,j+1}^{n} + n_{i,j-1}^{n} - 2\tilde{n}_{i,j}^{n}}{h_y^2} + C\tilde{n}_{i,j}^{n}\Bigg) \quad (11)$$

The LAX method has superior stability to the FTCS method, as the averaging helps dampen numerical instability, but it comes with the cost of reducing the accuracy. Since LAX averages neighboring grid points as part of the procedure, it artificially adds diffusive behavior to the differential equation it is modelling. This is not a huge issue as neutron diffusion is already clearly diffusive, but it does accelerate the diffusion beyond what the parameters reflect, making the result less accurate to the analytical solution even if the qualitative behavior is much the same.

The diffusive assumption produces sensible results everywhere except at the boundaries of our system, where special care must be taken to avoid over- or under- counting neutron density lost or gained.[4] In fact, boundary features that are trivially enforced by the full transport equations are nontrivial to enforce even in a time-independent version of the problem. Further, when applied in context of our time-dependent diffusion equation, the time-independent rules for more physically reasonable boundary conditions break down. As a result, we stick with Neumann and Dirichlet boundary conditions despite their inaccuracy to the full transport behavior.

Boundary conditions are implemented by creating a lattice that is two grid points larger than than the grid on which the solution is computed, with these grid points being defined to be certain values based on boundary conditions.

The diffusion equation can be solved analytically, with Dirichlet $\rho = 0$ boundary conditions being most convenient.

Our equation,

$$\frac{\partial}{\partial t}n(x,t) = D\nabla^2 n + Cn \quad (12)$$

can be solved via separation of variables. We begin with the ansatz $n(x,y,t) = X(x)Y(y)T(t)$, finding

$$XY\frac{\partial T}{\partial t} = D\Big(\frac{\partial^2 X}{\partial x^2}YT + X\frac{\partial^2 Y}{\partial y^2}T\Big) + C\,XYT \quad (13)$$

We then divide by XYT to find

$$\frac{\partial T}{\partial t}\frac{1}{T} = D\Big(\frac{\partial^2 X}{\partial x^2}\frac{1}{X} + \frac{\partial^2 Y}{\partial y^2}\frac{1}{Y}\Big) + C \quad (14)$$

Since the right hand side is time-independent, we can solve for $T(t)$ by labeling the entire right hand side as α.

$$\frac{\partial T}{\partial t}\frac{1}{T} = \alpha \rightarrow \frac{dT}{T} = \alpha\,dt \quad (15)$$

Integrating and exponentiating, we find

$$ln(T) = \alpha\,t \rightarrow T(t) = e^{\alpha\,t} \quad (16)$$

Yielding either exponential growth or decay depending on the sign of α.

The spatial portion, so far labeled alpha can be solved via another convenient relabeling of X and its derivatives as β and Y and its derivatives as γ.

$$\alpha - C = D\Big(\frac{\partial^2 X}{\partial x^2}\frac{1}{X} + \frac{\partial^2 Y}{\partial y^2}\frac{1}{Y}\Big) \quad (17)$$

$$\frac{\alpha - C}{D} = \frac{\partial^2 X}{\partial x^2}\frac{1}{X} + \frac{\partial^2 Y}{\partial y^2}\frac{1}{Y} = \beta + \gamma \quad (18)$$

$$\frac{\partial^2 X}{\partial x^2}\frac{1}{X} = \beta \rightarrow \frac{\partial^2 X}{\partial x^2} = \beta X \quad (19)$$

$$\frac{\partial^2 Y}{\partial y^2}\frac{1}{Y} =\rightarrow \frac{\partial^2 Y}{\partial y^2} = \gamma Y \quad (20)$$

Where

$$\beta = \frac{\alpha - C}{D} - \gamma \text{ and } \gamma = \frac{\alpha - C}{D} - \beta \quad (21)$$

The solutions for X and Y are sums of exponentials, and given the boundary conditions these must be sums

of sines and/or cosines. In fact, by enforcing boundary conditioons of $\rho = 0$ at $\pm\frac{L}{2}$, we can construct the solutions

$$X(x) = \sum_{j_x=1,\,2,\,3\ldots}^{\infty} a_{j_x} cos\left(\frac{\pi}{L_x} x(2j_x - 1)\right) \tag{22}$$

and

$$Y(y) = \sum_{j_y=1,\,2,\,3\ldots}^{\infty} a_{j_y} cos\left(\frac{\pi}{L_y} y(2j_y - 1)\right) \tag{23}$$

We can then take second derivatives of these expressions to find that

$$-\left[\frac{\pi}{L_x}(2J_x - 1)\right]^2 = \frac{\beta}{D} \text{ and } -\left[\frac{\pi}{L_y}(2J_y - 1)\right]^2 = \frac{\gamma}{D} \tag{24}$$

Rewriting together, we find $\beta + \gamma =$

$$\alpha_{j_x,j_y} = C - D\left(\left[\frac{\pi}{L_x}(2j_x - 1)\right]^2 + \left[\frac{\pi}{L_y}(2j_y - 1)\right]^2\right) \tag{25}$$

Which is the amplification factor of each spatial mode over time. If we simplify down to the mode with the lowest spatial frequency, which we can tell by inspection is necessarily larger than other spatial modes with higher j values, we find

$$\alpha_{1,1} = C - D\frac{\pi^2}{L_x^2} - D\frac{\pi^2}{L_y^2} \tag{26}$$

Which, if we put the box in terms of its aspect ratio, r, and write $L_x = rL_y$, becomes

$$\alpha_{1,1} = C - D\pi^2\left(\frac{1}{L_y^2 r^2} + \frac{r^2}{L_y^2 r^2}\right) \tag{27}$$

$$\alpha_{1,1} = C - D\pi^2\left(\frac{1 + r^2}{L_y^2 r^2}\right) \tag{28}$$

Which for the aspect ratio of 1, the situation used in our numerical simulations reduces via $L_x = L_y = L$ to

$$\alpha_{1,1} = C - 2D\frac{\pi^2}{L^2} \tag{29}$$

Which we can use to inform what amplification factor our solution should have based on the constants in our model and the size of our square box.

If we solve for the critical length, where $\alpha = 0$, we find

$$L_c = \pi\sqrt{\frac{2D}{C}} \tag{30}$$

Even slightly above this side length, the neutron density should rise exponentially, and slightly below L_c, it should fall exponentially towards zero.

III. RESULTS

For numerical simulations of neutron diffusion, the FTCS and LAX methods were used. All simulations were performed in a square domain of side length $L = 10$, with neutron creation constant $C = 1$, and with diffusion constant $D = 1$. The initial neutron density profile given was a Gaussian distribution centered within the domain with amplitude $A = 1$ and standard deviation $\sigma = 1$. Simulations were run for 15 simulated "seconds", as this was long enough for stationary spatial distributions and growth behavior to become clear. Simulating exponential growth for too long would make floating point precision errors appear, but $t_{max} = 15$ was short enough to avoid this. The number of grid points along each axis was $N = 102$, with the first and last grid points being determined via boundary conditions, leaving 100 points along each dimension to be determined by the numerical scheme. Various time steps τ were used. For FTCS, the stability criterion dictated that tau be at most

$$\tau_{FTCS} \leq \frac{h_x^2 h_y^2}{2D(h_x^2 + h_y^2)} \to \frac{h^2}{4D} \tag{31}$$

for simple diffusion, which seems to give good results for neutron diffusion when implemented [5].

The LAX method seems to have more lenient stability conditions in exchange for decreased accuracy, though we have not derived the precise stability conditions. By increasing the time step, the model accuracy decreased significantly even while the scheme remained stable. With $\tau = 0.004$, slightly above the stability criterion for FTCS, we get a blowup in the FTCS method but a LAX solution that remains stable. This behavior is shown in Figure 1. With a sufficiently small time step, LAX and FTCS look essentially identical.

For Dirichlet $\rho = 0$ boundary conditions, the spatial distribution of neutron density approaches its most stable configuration. This configuration is seen to be the analytical solution: a sum of cosine waves along each dimension. Since the diffusion equation disperses high frequency components, the lowest frequency that

Fig. 1. Stability Comparison

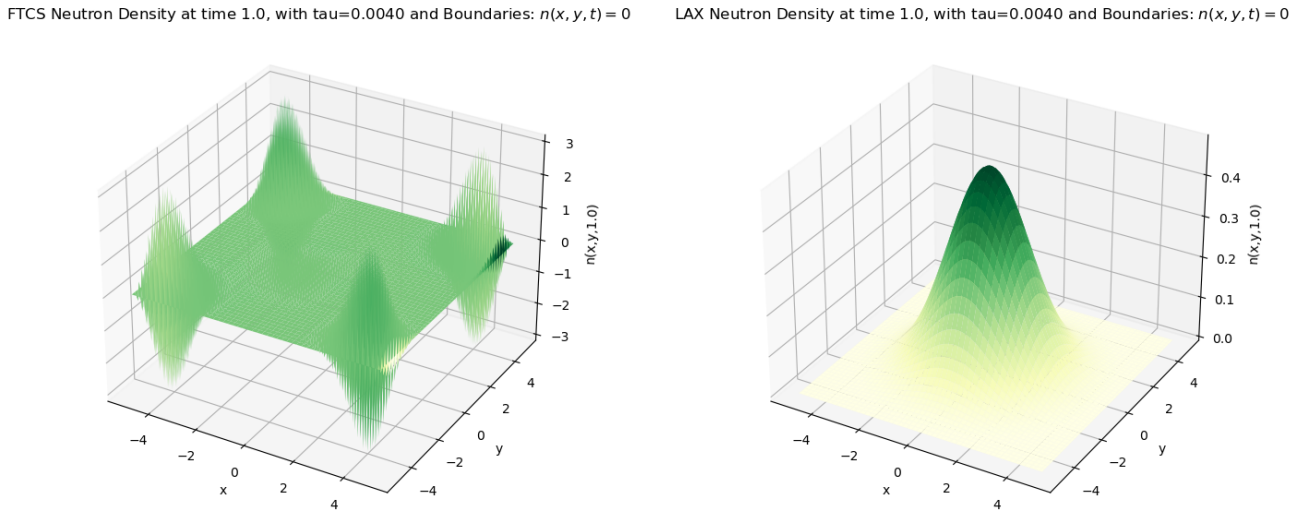

(a) FTCS blows up with τ =0.004.

(b) LAX remains stable with τ =0.004.

Fig. 2. Dirichlet Solution

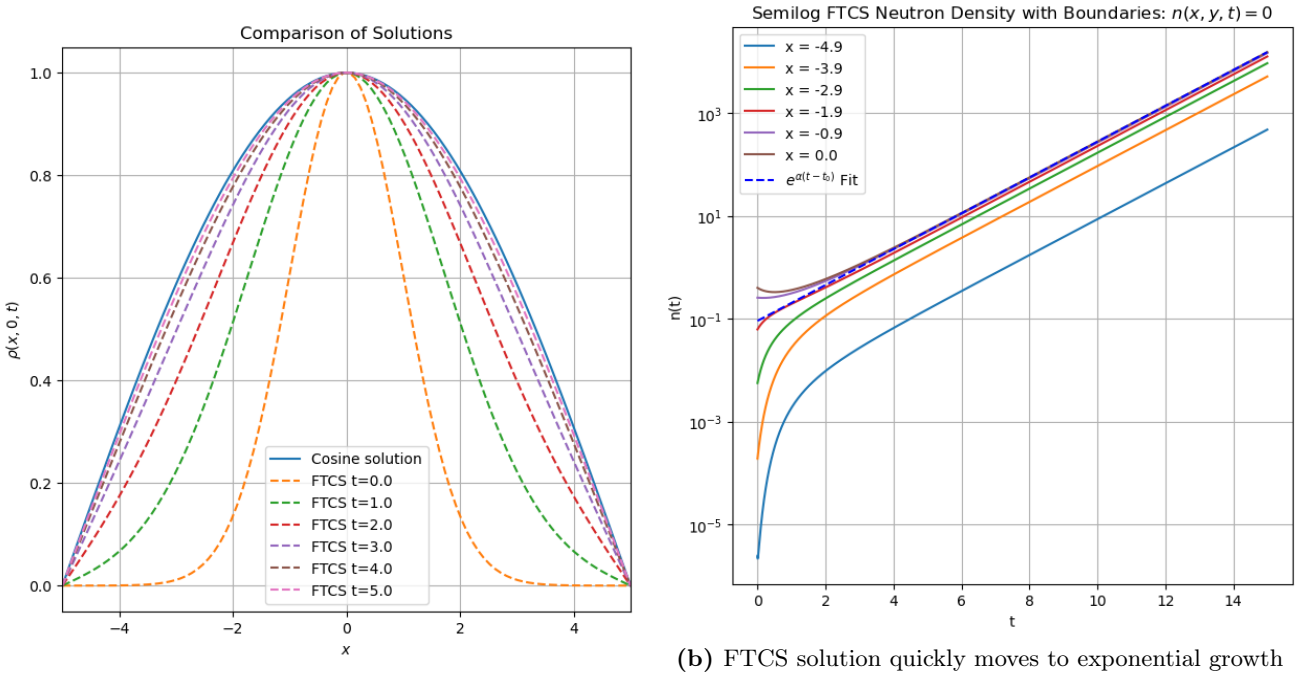

(a) FTCS solutions with normalized amplitudes approach the analytical cosine solution for the Dirichlet boundary conditions of $\rho = 0$.

(b) FTCS solution quickly moves to exponential growth once diffusion stops significantly changing the spatial distribution. These points are taken along a spatial slice closest on the grid to y = 0.

can fit in the domain is the stable solution, and that is this minimal cosine distribution seen in Figure 2a.

The time-dependent portion of the solution also fits the analytical solution well, as the exponential growth of the amplitude is clearly present. An interesting behavior is the delay before different parts of the domain begin their exponential growth phase. Points near the center initially dip in amplitude as their neutron density is diffused to fill the domain, while points near the edge have above-exponential growth due to the diffused neutron density reaching them being very large relative to their starting neutron density. Fitting the growth of the neutron density at the grid point closest to the center to a time-delayed exponential,

$$\rho(t) = e^{\alpha(t-t_0)} \tag{32}$$

we find the time delay to be 3 seconds and the exponential growth constant to be $\alpha = 0.8022$. The predicted value of α from equation 29 is 0.8026, so this provides good agreement between the numerical and analytical solutions. This exponential growth constant holds for every point of the solution once the diffusion process reaches a stationary shape, as shown in Figure 2b, and seems to start for a given point once the neutron density there becomes concave down.

For the Neumann boundary conditions of zero spatial derivative, the neutron density is guaranteed to be supercritical, as no density is lost at the boundaries. As a result of the differing boundary conditions, we find different solutions in the spatial coordinates alongside a faster exponential growth constant. For an identical initial spatial distribution as before, α is found to be 0.994, with a longer initial delay of 3.6 seconds.

The solutions look markedly different due to the boundary conditions allowing a nonzero value at the boundaries, which leads to different Fourier modes in spatial distribution. One could have imagined seeing a completely flat distribution, as in the regular diffusion equation, but this is not quite what is observed. I initially believed this to be because the source term's dependence on the neutron density at each point acted to preserve peaks and troughs in density that ordinary diffusion would flatten. However, upon closer inspection, the distribution does indeed flatten, just in a relative sense that the automatic axes of my visualizations obscured. While initially, the difference between the peak amplitude and the edge amplitude is 100% of the peak amplitude (as the edges start at zero), this falls quickly with time. In Figure 3a, the edges are only about 10% lower than the peak amplitude, and this *relative* difference decreases with time even as its absolute density difference increases. The relative flattening is even more clear in Figure 3b, where it can be seen that all spatial points converge to a single exponential growth curve, with their relative differences in amplitude becoming irrelevant on a logarithmic scale. This is in direct contrast to the Dirichlet case seen in Figure 2b, where the boundary conditions enforce that the solution follows a cosine in space, which keeps the exponential growth curves split even while they have the same growth constant.

IV. CONCLUSION

While a diffusion model of neutron flux is too simple to model physically reasonable nuclear reactors, it provides a good use case for numerical methods. Both the FTCS and LAX methods function well for simulating neutron diffusion, though each with a different accuracy-stability trade-off. Using a time step dictated by the FTCS stability criterion was sufficient to prevent blowup, as expected, with Equation 31 providing the correct limit.

For Dirichlet boundary conditions of $\rho = 0$, the numerical solution was in agreement with the analytical superposition of cosines solution, and quickly evolved to the simplest single-cosine solution due to diffusion. The exponential growth constant found numerically $\alpha = 0.8022$ also agreed very well with the analytical value of $\alpha = 0.8026$. The delay of $t_0 = 3$ seconds was also sensible given the initial primarily-diffusive spreading behavior of the Gaussian initial condition.

For Neumann boundary conditions of zero derivative, the spatial distribution was found to flatten considerably as a percentage of peak amplitude, but retain some spatial variation from the Gaussian initial conditions. The exponential growth constant for the Neumann case was found to be $\alpha = 0.994$, sensibly higher given that neutron density is reflected at the boundaries rather than lost as under Dirichlet boundary conditions.

Investigating the analytical solution for Neumann boundary conditions in future works would likely be fruitful for gaining better understanding the spatial distribution at both short and long times. Analysis via Fourier methods would also provide a greater understanding of spatial distributions for both sets of boundary conditions.

Fig. 3. Neumann Solution

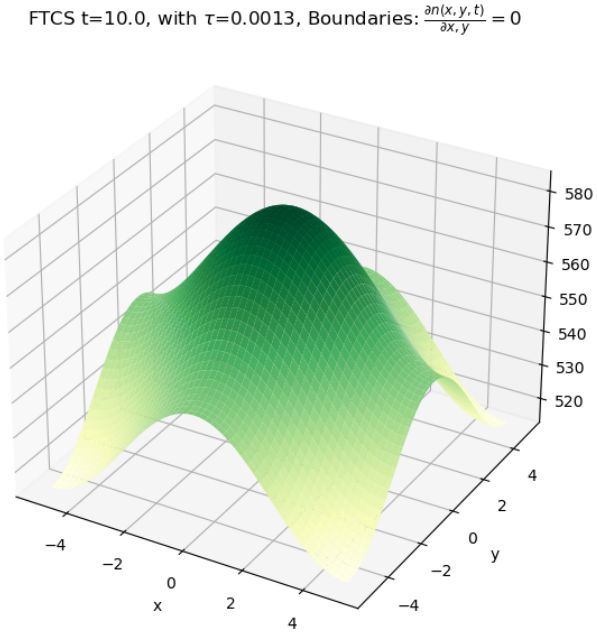

(a) Approximate FTCS spatial solution for the Neumann boundary conditions of $\frac{\partial \rho}{\partial x,y} = 0$.

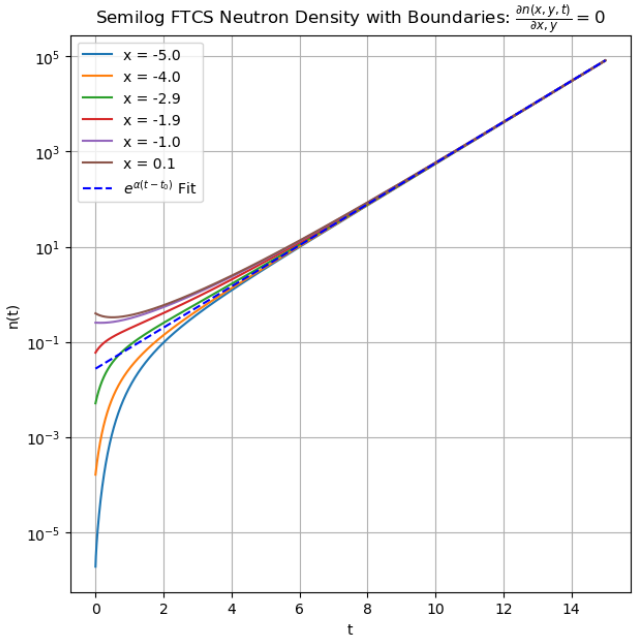

(b) FTCS solution quickly moves to exponential growth once diffusion stops significantly changing the spatial distribution, as before. The rate of this growth, however, is higher.

REFERENCES

[1] Alejandro L. Garcia. *Numerical Methods for Physics (Python)*. (CreateSpace Independent Publishing, 2017).

[2] Stacey, W. M. *Nuclear Reactor Physics*. (Wiley-VCH, 2007).

[3] Lewis, E. E. *Fundamentals of Nuclear Reactor Physics*. (Elsevier, 2008).

[4] Noh, T. A Study on Diffusion Approximations to Neutron Transport Boundary Conditions. *J. of Nucl. Fuel Cycle and waste Technol.* **16**, 203–209 (2018).

[5] Moin, P. *Fundamentals of engineering numerical analysis*. (Cambridge University Press, 2010).